JACS
JOURNAL OF THE AMERICAN CHEMICAL SOCIETY
Article
pubs.acs.org/JACS

Generation of Candidate Ligands for Nicotinic Acetylcholine Receptors via in situ Click Chemistry with a Soluble Acetylcholine Binding Protein Template

Neil P. Grimster,[†] Bernhard Stump,[†] Joseph R. Fotsing,[†] Timo Weide,[†] Todd T. Talley,[‡] John G. Yamauchi,[‡] Ákos Nemecz,[‡,§] Choel Kim,[∥] Kwok-Yiu Ho,[‡] K. Barry Sharpless,[†] Palmer Taylor,[‡] and Valery V. Fokin*[,†]

[†]Skaggs Institute for Chemical Biology, The Scripps Research Institute, 10550 North Torrey Pines Road, La Jolla, California 92037, United States

[‡]Department of Pharmacology, Skaggs School of Pharmacy & Pharmaceutical Sciences, and [§]Department of Chemistry and Biochemistry, University of California San Diego, La Jolla, California 92093, United States

[∥]Department of Pharmacology, The Verna and Marrs McLean Department of Biochemistry and Molecular Biology, Baylor College of Medicine, Houston, Texas 77030, United States

Supporting Information

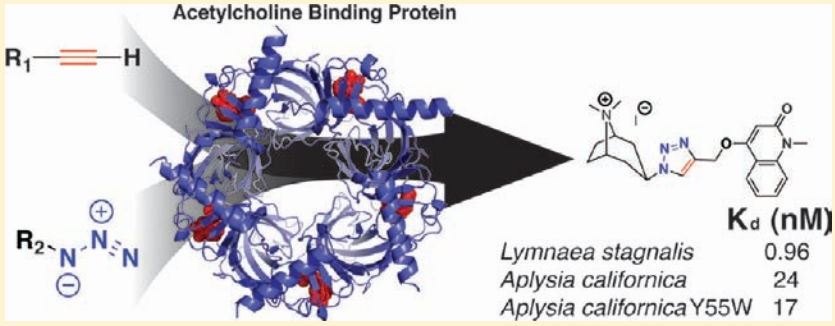

ABSTRACT: Nicotinic acetylcholine receptors (nAChRs), which are responsible for mediating key physiological functions, are ubiquitous in the central and peripheral nervous systems. As members of the Cys loop ligand-gated ion channel family, neuronal nAChRs are pentameric, composed of various permutations of α (α2 to α10) and β (β2 to β4) subunits forming functional heteromeric or homomeric receptors. Diversity in nAChR subunit composition complicates the development of selective ligands for specific subtypes, since the five binding sites reside at the subunit interfaces. The acetylcholine binding protein (AChBP), a soluble extracellular domain homologue secreted by mollusks, serves as a general structural surrogate for the nAChRs. In this work, homomeric AChBPs from *Lymnaea* and *Aplysia* snails were used as in situ templates for the generation of novel and potent ligands that selectively bind to these proteins. The cycloaddition reaction between building-block azides and alkynes to form stable 1,2,3-triazoles was used to generate the leads. The extent of triazole formation on the AChBP template correlated with the affinity of the triazole product for the nicotinic ligand binding site. Instead of the in situ protein-templated azide−alkyne cycloaddition reaction occurring at a localized, sequestered enzyme active center as previously shown, we demonstrate that the in situ reaction can take place at the subunit interfaces of an oligomeric protein and can thus be used as a tool for identifying novel candidate nAChR ligands. The crystal structure of one of the in situ-formed triazole−AChBP complexes shows binding poses and molecular determinants of interactions predicted from structures of known agonists and antagonists. Hence, the click chemistry approach with an in situ template of a receptor provides a novel synthetic avenue for generating candidate agonists and antagonists for ligand-gated ion channels.

1. INTRODUCTION

Nicotinic acetylcholine receptors (nAChRs) belong to a superfamily of neurotransmitter ligand-gated ion channels characterized by a pentameric structure of Cys-loop-containing subunits.[1,2] This family of proteins is actuated upon binding of a specific ligand and includes other key neurotransmitter receptors, such as glycine, GABA-A, and 5-HT_3 types.[3] The nAChRs are currently being considered as therapeutic targets for central nervous system disorders such as schizophrenia, nicotine addiction, and Alzheimer's disease among other cognitive disorders.[2,4,5] An extensive variety of synthetic and naturally occurring ligands for nAChRs of variable selectivity are known. Agonists and competitive antagonists bind in the

Received: January 7, 2012
Published: March 6, 2012

dx.doi.org/10.1021/ja3001858 | J. Am. Chem. Soc. 2012, 134, 6732−6740

extracellular domain at the interface between subunits, and agonists transmit ligand occupation through conformational changes to open an internally located ion channel, effecting a rapid depolarization.[1,6]

The acetylcholine binding proteins (AChBPs), which are homologous to the extracellular domain of pentameric ligand-gated ion channels, have been found to be expressed as soluble pentamers in select gastropods and polychaetes.[7−11] Homologous to the N-terminal ∼210 amino acids in the extracellular receptor domain, AChBPs mimic the recognition properties of nAChRs, providing a critical template describing the shape and spatial disposition of residues contributing to the binding site.[7,12] The five acetylcholine binding sites of the AChBPs lie at the subunit interfaces and are partially surrounded by a flexible loop C found between sheets β9 and β10 that extends across the subunit interface.

Structure-based drug design and screening of compound libraries have been a laborious task in the case of nAChRs. The membrane disposition of the nAChR, the diversity of receptor subtypes, and the dynamic nature of the binding site complicate classical drug discovery approaches. In contrast, target-guided in situ synthesis is an attractive and efficient approach to drug discovery because it directly employs the biological target for the assembly of candidate leads from their own building blocks. Independent of the knowledge of the geometry of the protein target, it allows fast screening of potential ligands whose building blocks are "templated" by the target protein. Although this concept has been previously demonstrated using different connecting reactions,[13−16] the in situ click chemistry approach is unique with its reliance upon the nearly bioorthogonal 1,3-dipolar cycloaddition between azides and alkynes, a reaction that is fully compatible with functional groups found in normal physiological environments.

These building blocks readily react with each other when in proximity but remain inert toward side chains and amide backbones of proteins. This highly exergonic reaction produces five-membered nitrogen heterocycles, *anti*- or *syn*-1,2,3-triazoles, that are stable toward acidic and basic hydrolysis as well as under severe redox conditions.[17] A target protein, employed as a template, can generate a high-affinity ligand from monovalent building blocks using the in situ click chemistry approach.[18] The process begins with selective binding of anchor molecules to specific areas of the protein binding site. Subsequently, if two of the bound anchor molecules are in proximity, they link together irreversibly within the confines of their binding pockets and thereby allow the formation of an energetically more favorable new complex with the protein. The resultant compound can then be detected by liquid chromatography/mass spectrometry (LC/MS).

Since this approach employs the biological target to assemble its own ligands from a library of reagents that can be combined in a multitude of different ways,[18] rather than requiring the synthesis, purification, and screening of each possible library product, the use of in situ click chemistry promises greater efficiency than traditional combinatorial chemistry or fragment-based drug design. Moreover, the triazole product may induce or select a conformation of the macromolecule so adapted in conformation to the binding of the ligand.[19] The template-generated compounds are then further screened to assess their binding affinity and specificity for the target.

In this work, we used AChBPs from *Lymnaea stagnalis* (*Ls*), *Aplysia californica* (*Ac*), and the Y55W *Aplysia* mutant (*Ac*Y55W) as template surrogates for nAChRs. Because of the dynamic molecular motion of the protein subunit interface, in situ click chemistry facilitates the identification of potential ligands for different conformational states of a protein without the need to synthesize large screening libraries. We initially prepared an artificial triazole-containing AChBP ligand via Cu(I)-catalyzed azide−alkyne cycloaddition (CuAAC) conditions,[20,21] and after confirmation of the triazole's affinity, we subsequently utilized the compound's components to validate the AChBPs as in situ click chemistry templates. The alkyne component and subsequent in situ azide component that formed the product with higher efficiency and affinity were then used as leads for the refinement of building blocks to form triazole structures. These derivatives should mimic the properties of the natural nAChR neurotransmitter, acetylcholine (ACh), along with naturally occurring and synthetic congeners, thereby providing a starting point for developing selective ligands that address the binding site. Furthermore, we demonstrate that multiple ligands may be formed when a mixture of building blocks is screened simultaneously, with the amount of the triazole product generated by the template being proportional to its affinity for the binding site. Structurally we demonstrate in situ product formation at a subunit interface binding region of a multisubunit protein, the AChBP. This receptor surrogate serves as a template for the generation of nicotinic receptor ligands.

2. EXPERIMENTAL METHODS

Synthetic Compound Preparations. All azides were synthesized by the displacement of either a halide, mesylate, or tosylate with sodium azide in *N*,*N*-dimethylformamide. Propargyl phenol ethers were prepared using literature conditions.[22] The 1,4-triazole products **2**, **14**, **15**, **18**, **19**, **27**, **28**, and **29** were synthesized using CuAAC, whereas 1,5-triazole **18a** was synthesized using ruthenium-catalyzed azide−alkyne cycloaddition (RuAAC;[23,24] see the Supporting Information for details).

Procedure for the in situ Formation of 2 from a Binary-Component Mixture. Azide **4** [1 μL, 100 mM in 0.1 M aqueous sodium phosphate buffer, pH 7.0 (PBS)] was added to 98 μL of a solution of the protein of interest (∼1 mg/mL in PBS) in a microfuge tube, followed immediately by alkyne **3** [1 μL, 50 mM in dimethyl sulfoxide (DMSO)] to give final concentrations of 1 mM for azide **4** and 0.5 mM for alkyne **3**. The reaction mixture was briefly vortexed and then incubated at room temperature. In a separate microfuge tube, azide **4** (1 μL, 100 mM in PBS) and alkyne **3** (1 μL, 50 mM in DMSO) were diluted with water (87 μL) before aqueous copper sulfate (1 μL, 0.05 M) and aqueous sodium ascorbate (10 μL, 0.1 M) were added. The reaction mixture was briefly vortexed and then incubated at room temperature. After 3 days, three samples (25 μL) from each tube were directly injected into the LC/MS instrument to perform LC/MS-SIM analysis under the following conditions: Zorbax 4.6 mm × 3 cm, SB-C18 (rapid resolution) reversed-phase column preceded by a Phenomenex C18 guard column; flow rate, 0.5 mL/min; gradient elution, (H_2O + 0.05% TFA)/(MeCN + 0.05% TFA) from 100:0 to 0:100 over 15 min followed by 100% MeCN + 0.05% TFA for 5 min with a post-run time of 5 min using the starting solvent ratio. Detection was by electrospray ionization and mass spectrometric detection with positive selected-ion monitoring tuned to the molecular mass of **2** (M+). The cycloaddition product was identified by comparison of its retention time with those determined from analysis of the copper-catalyzed reaction and by its molecular weight. Control experiments in the presence of bovine serum albumin (BSA, 1 mg/mL) instead of the binding protein as well as in the presence of *Ls* and the known receptor inhibitor methyllycaconitine (MLA, 1 mM final concentration) were run as described above.

Procedure for the in situ Screening of Single-Component Libraries. To generate library **1a**, azides **4**−**8** were dissolved in PBS (100 mM) and the solutions combined. The solution of azides (1 μL)

dx.doi.org/10.1021/ja3001858 | J. Am. Chem. Soc. 2012, 134, 6732−6740

was added to the protein of interest (~1 mg/mL in PBS, 98 μL) in a microfuge tube, followed immediately by alkyne **3** (1 μL, 50 mM in DMSO). The reaction and controls were performed similarly to the binary component mixture. After 3 days, the reactions were analyzed in triplicate as described for the binary mixture, using mass spectroscopic detection with positive selected-ion monitoring tuned to the five expected molecular masses of the products (M+). The cycloaddition products were identified by comparison of the retention times with those determined from the analysis of the copper-catalyzed reaction and by their molecular weights. Azide library **1b** was screened using in situ click chemistry as described above, substituting azides **4**–**8** with azides **9**–**13**. The alkyne library was again screened as described above, using azide **9** (100 mM in PBS) and a combined DMSO solution of alkynes **3** and **23**–**26** at a final concentration of 0.5 mM.

Procedure for the in situ Screening of Azide and Alkyne Libraries. Azides **4**–**13** were dissolved separately in PBS (100 mM), and 25 μL aliquots of these solutions were taken and combined. Alkynes **3** and **23**–**26** were dissolved in DMSO (50 mM) and the solutions combined. The combined solution of azides (10 μL) was added to a solution of *Ls* (~1 mg/mL in PBS, 980 μL) in a microfuge tube, followed immediately by the combined solution of alkynes (10 μL). The reaction mixture was briefly vortexed and then incubated at room temperature. After 10 days, triplicate analysis of the protein-catalyzed reaction was performed using the chromatography conditions described above. To improve the MS detection sensitivity, 10 injections (each 25 μL) were performed; each injection was tuned to detect five of the expected 50 molecular weights. A control experiment in the presence of BSA (1 mg/mL) instead of the binding protein was performed. As some of the potential in situ click chemistry products have the same molecular weights, the corresponding triazoles were prepared by reacting each azide with the five alkynes under CuAAC conditions. Therefore, azides **4**–**13** (1 μL, 100 mM in PBS) were charged to 10 separate microfuge tubes, and water (87 μL), combined alkyne solution (1 μL) as described above, aqueous copper sulfate (1 μL, 0.05 M) and aqueous sodium ascorbate (10 μL, 0.1 M) were added. The reaction mixtures were briefly vortexed and then incubated at room temperature. After 10 days, analyses of the copper-catalyzed reactions were performed as described above. The cycloaddition products of the in situ screen were identified by their molecular weights and by comparison of the retention times of the formed products with the values determined by analysis of the copper-catalyzed reactions.

Preparation of AChBPs. The AChBPs from *Ls*, *Ac*, and *Ac*Y55W were expressed and purified as previously described.[25,26] Briefly, AChBPs were expressed with an amino-terminal FLAG epitope tag and secreted from stably transfected HEK293S cells lacking the *N*-acetylglucosaminyltransferase I (GnTI$^-$) gene.[27] The protein was purified with FLAG-antibody resin and eluted with FLAG peptide (Sigma). The affinity-purified protein was further characterized by size-exclusion chromatography [Superose 6 10/300 GL column (GE Healthcare) in 50 mM Tris-HCl (pH 7.4), 150 mM NaCl, 0.02% NaN_3] to ascertain the pentameric association. Purified AChBP pentamers were then concentrated in a YM50 Centricon ultrafiltration unit (Millipore) to a final concentration of ~5 mg/mL, removing monomeric subunits and trace contaminants.

Radioligand Binding Assays. A scintillation proximity assay (SPA) was used to determine the apparent K_d value of the compounds as reported previously.[26] Briefly, AChBP (0.5–1.0 nM final concentration in binding sites), polyvinyltoluene anti-mouse SPA scintillation beads (0.17 mg/mL final concentration, GE Healthcare), monoclonal anti-FLAG M2 antibody from mouse 1:8000 dilution (Sigma), and (±)-[^{3}H]epibatidine (5–20 nM final concentration, GE Healthcare) were combined with PBS. A quick screen was performed to determine the relative binding affinities of the compounds by adding compound to the previously mentioned solution at a final concentration of 10 μM. Apparent K_d values were then determined for compounds that reduced the normalized counts per minute below 50%. Saturation binding of (±)-[^{3}H]epibatidine was measured by adding increasing concentrations of (±)-[^{3}H]epibatidine in a constant volume. Nonspecific binding was determined in parallel by adding a saturating concentration (12.5 μM) of MLA (Tocris) to an identical set of samples. Competition assays were conducted in a similar manner except that the concentration of (±)-[^{3}H]epibatidine was held constant (5–20 nM final concentration) and varying concentrations of competing ligand were added to the samples in a constant volume, of either 50 μl or 100 μl. The resulting mixtures were allowed to equilibrate at room temperature for a minimum of 1 h and measured on a 1450 MicroBeta TriLux liquid scintillation counter (Wallac). The data obtained were normalized, and the K_d was calculated from the observed EC_{50} value[28] using GraphPad Prism version 4.02 (GraphPad Software, San Diego, CA, USA, www.graphpad.com). At least three independent experiments performed in duplicate were used to determine the reported K_d values.

Complex Formation and Crystallization. The **18**–*Ac* AChBP complex was formed by combining 2 μL of a solution of **18** (10 mmol dissolved in DMSO) with 48 μL of purified concentrated protein at a concentration of 5 mg/mL to achieve a stoichiometric excess of ligand to binding sites. The **18**–*Ac* AChBP complex cocrystals were prepared by the vapor diffusion hanging drop method. Concentrated protein complex was mixed in a 1 μL/1 μL ratio with a solution consisting of 0.1 M Tris-HCl (pH 8.0), 0.25 M $MgCl_2$, and 20% (w/v) PEG 4000; the mixture was incubated at 22 °C and suspended over 500 μL of the solution. Crystals of final size 0.3 mm × 0.3 mm × 0.2 mm appeared after a few weeks.

X-ray Diffraction Data Collection. **18**–*Ac* AChBP complex cocrystals were transferred to a cryoprotective harvest solution [0.1 M Tris-HCl (pH 8.0), 0.25 M $MgCl_2$, 12% (w/v) PEG 4000, and 10% (v/v) glycerol] and flash-cooled directly in liquid nitrogen. A full set of X-ray diffraction data was collected at 100 K on ALS beamline 8.2.2 at Lawrence Berkeley National Laboratory. The data were processed using the HKL2000 program.[29] Data collection statistics are given in Table S7 in the Supporting Information.

Structure Refinement. The **18**–*Ac* AChBP complex structure was solved by the molecular replacement method with the PHASER[30] software using an ensemble of AChBP structures (PDB entries 2BYN, 2PGZ, 2BYP, 2BYR, 2BYS, and 3C79) as the search model. The electron density maps were fitted with COOT,[31] and structure refinement used the program REFMAC5.[32] Refinement statistics are listed in Table S7. Atomic coordinates and structure factors of the complex have been deposited in the Protein Data Bank (PDB entry 4DBM). The structural figures were generated using PyMOL[33] and Discovery Studio 3.0 (Accelrys).

3. RESULTS

We hypothesized that substituting a 1,2,3-triazole unit for the ester moiety of ACh would mimic its hydrogen-bond-acceptor character (Figure 1), an interaction that has previously been observed in triazole-containing peptidomimetics.[34–36] Furthermore, the conservation of the trimethylammonium-containing moiety of ACh would maintain the crucial cation–π interaction with Trp147 (*Ac* AChBP numbering) and other proximal aromatic amino acid side chains.[25,37–40]

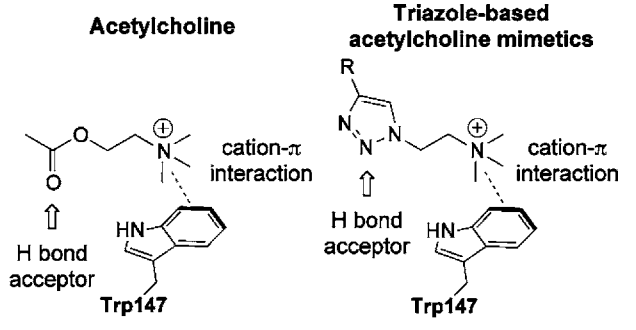

Figure 1. Binding pose of acetylcholine (left) and proposed binding pose of the triazole-based acetylcholine mimetic (right).

dx.doi.org/10.1021/ja3001858 | J. Am. Chem. Soc. 2012, 134, 6732–6740

In conformance with our hypothesis, azide **1** was reacted with a range of alkynes under standard CuAAC reaction conditions, and the resultant tertiary amines were quaternized with methyl iodide (eq 1 in Scheme 1). Screening of the

Scheme 1. Synthesis of a Triazole Library Using Standard CuAAC Reaction Conditions

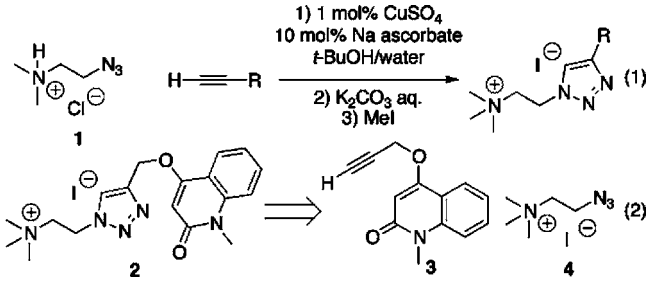

compounds (data not shown) against *Ac*, *Ls*, and *Ac*Y55W AChBPs identified compound **2** as having a relatively strong association with all three AChR surrogates (Table 1).

Table 1. Proof of Concept: Amounts of Triazole 2 Formed in situ in the Presence of AChBP Templates Compared with the Respective Affinities of the Triazole Product

AChBP species	MS counts[2]	K_d [nM]	Affinity [μM^{-1}]	Structure[3]	#
Ls	100.0 ± 0.3	75 ± 26	13	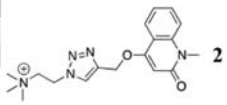	2
Ac	8.0 ±0.1	1900± 800	0.53		
*Ac*Y55W	8.9 ±0.2	370± 50	2.7		
Ls + MLA	2.8 ±0.0	n/a	n/a		
BSA[1]	2.8 ±0.1	n/a	n/a		

[1] BSA control protein was used in place of the AChBP template. [2] MS counts were corrected for background via BSA controls and normalized to *Ls*. [3] Structure of the cation detected by MS.

We first wanted to confirm that the flexible subunit interfaces in the AChBPs were capable of catalyzing the formation of **2** in situ, as most previous examples have relied upon well-defined sites internal to the subunit.[41] To validate our hypothesis, the constituent alkyne **3** and azide **4** (eq 2 in Scheme 1) were incubated in the presence of *Ls*, *Ac*, and *Ac*Y55W AChBPs in PBS at room temperature for 3 days (see Experimental Methods). In addition, two control reactions were performed: incubation of the reactants in the presence of BSA, to determine whether nonspecific protein catalysis of the triazole-forming cycloaddition was occurring; and incubation in the presence of *Ls* with a known competing ligand, MLA, to confirm that the protein-templated reaction was occurring at the ACh orthosteric binding site.

Triplicate samples of the reaction mixtures were analyzed by LC/MS with selected-ion monitoring (detection window set to the molecular weight corresponding to the most abundant peak), and the retention times were compared with those of the previously synthesized sample of **2**. Analysis of these data showed that *Ls* efficiently templated the formation of ligand **2** under the reaction conditions, while both *Ac* and *Ac*Y55W AChBP also produced the product, but much less efficiently (Table 1).

Comparison of the in situ click chemistry reactions performed in the presence of AChBPs with the BSA control reaction confirmed that triazole formation was selectively accelerated in the presence of the receptor surrogates. The control reaction showed that MLA, a nicotinic antagonist, returned the product formation to background levels, thus demonstrating that the flexible subunit interface ACh binding site indeed served as the template for the cycloaddition reaction. It is noted that the amounts of product formed in the presence of the template were correlated with the affinities ($1/K_d$, μM^{-1}) determined for the tested AChBPs. This suggests that product selectivity toward a specific target over closely related receptor subtypes could be inferred from the bioorthogonal triazole formation without the need to acquire individual binding data. Unfortunately, the 1,4- (*anti*-) and 1,5- (*syn*-) 1,2,3-triazole isomers proved to be inseparable by LC/MS, despite considerable method development. Thus, subsequent experiments considered both regioisomers together, while comparisons were made to the 1,4-isomers because of their ease of synthesis via CuAAC.[20,21] The outcome of the in situ triazole templation at a flexible binding site expands the templation potential of in situ click chemistry to receptor-relevant targets and intersubunit binding sites.

Triazole **2**, the in situ-formed ligand with the dissociation constant in the nanomolar range for *Ls*, was next used as a lead for the discovery of analogues with improved affinity and selectivity for the closely related AChBPs. Selective target-catalyzed synthesis of a new ligand from a library of building blocks simultaneously present in a single reaction mixture would be a significant advantage in drug discovery, enabling rapid screening of many building-block pools or combinations and reducing the amount of protein required for each individual analysis. To this end, azide building blocks containing a variety of quaternary nitrogen centers were synthesized (Table 2). This

Table 2. Azide Libraries 1a and 1b: in situ Click Chemistry Screen against Alkyne 3

Library	Azides					Alkyne
1a	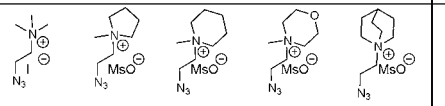					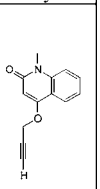
	4	**5**	**6**	**7**	**8**	**3**
1b	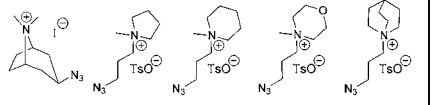					
	9	**10**	**11**	**12**	**13**	

library was designed to probe the effect of the quaternary amine systematically using ring systems of increasing complexity (**4**–**8**, library **1a**; and **9**, library **1b**; Table 2) while also extending the linker between the azide and the amine for each iterative compound (**10**–**13**, library **1b**; Table 2).

The in situ reactions for libraries **1a** and **1b** were allowed to proceed at room temperature for 3 days. LC/MS analysis of the reaction mixtures (performed in triplicate) revealed several interesting phenomena (Tables 3a and 3b). As demonstrated above, *Ls* catalyzed the formation of the triazole products more efficiently than the *Ac* and *Ac*Y55W AChBPs, while no products were detected in the BSA control reaction. However, in contrast to the binary mixture, there was no pronounced increase in the formation of triazole **2** when library **1a** was used. This finding can be explained by the preferential binding of azides **6** and **8** to the template, favoring the formation of products **15** and **14**, respectively.[42] These compounds were synthesized via CuAAC, and their K_d values were determined. Comparison of the amounts of product formed in situ with the

dx.doi.org/10.1021/ja3001858 | *J. Am. Chem. Soc.* 2012, 134, 6732–6740

Table 3a. Templation and Binding Data for the Triazole Derivatives of the in situ Click Chemistry Screen of Azide Building Blocks (Library 1a)

AChBP species	MS counts[1]	K_d [nM]	Affinity [μM^{-1}]	Structure[3]	#
Ls	3.8 ± 0.1	75 ± 26	13	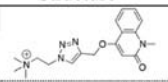	**2**
Ac	0.0	1900 ± 800	0.53		
*Ac*Y55W	0.0	370 ± 50	2.7		
Ls	100 ± 2.4	9 ± 0.4	110	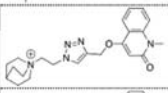	**14**
Ac	8.0 ± 0.1	120 ± 25	8.3		
*Ac*Y55W	15.9 ± 0.1	88 ± 4.2	11		
Ls	97.3 ± 3.3	10 ± 1.7	100	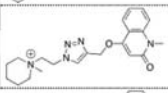	**15**
Ac	10.1 ± 0.0	210 ± 46	4.8		
*Ac*Y55W	12.8 ± 0.2	50 ± 4.7	20		
Ls	26.7 ± 0.6	n.d.[2]	n.d.	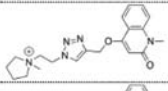	**16**
Ac	5.6 ± 0.1	n.d.	n.d.		
*Ac*Y55W	3.9 ±1.7	n.d.	n.d.		
Ls	0.0	n.d.	n.d.	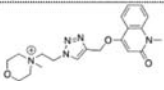	**17**
Ac	0.0	n.d.	n.d.		
*Ac*Y55W	0.0	n.d.	n.d.		

[1] MS counts were corrected for background via BSA controls and normalized. [2] n.d. represents no data, as the compound was not synthesized to generate affinity values. [3] Structures of the cations detected by MS.

Table 3b. Templation and Binding Data for the Triazole Derivatives of the in situ Click Chemistry Screen of Azide Building Blocks (Library 1b)

AChBP species	MS counts[1]	K_d [nM]	Affinity [μM^{-1}]	Structure[3]	#
Ls	100.0 ± 0.5	0.96 ± 0.22	1040	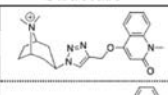	**18**
Ac	14.3 ± 0.1	24 ± 6.8	42		
*Ac*Y55W	13.3 ± 0.3	17 ± 4.8	59		
Ls	40.0 ± 1.5	82 ± 14	12	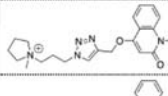	**19**
Ac	13.3 ± 0.5	470 ± 65	2.1		
*Ac*Y55W	12.3 ± 0.3	280 ± 21	3.6		
Ls	29.2 ± 1.1	n.d.[2]	n.d.	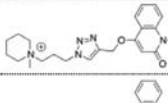	**20**
Ac	14.1 ± 0.3	n.d.	n.d.		
*Ac*Y55W	14.8 ± 0.3	n.d.	n.d.		
Ls	0.0	n.d.	n.d.	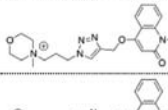	**21**
Ac	0.0	n.d.	n.d.		
*Ac*Y55W	0.0	n.d.	n.d.		
Ls	28.4 ± 0.7	n.d.	n.d.	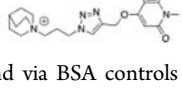	**22**
Ac	8.0 ± 0.2	n.d.	n.d.		
*Ac*Y55W	12.1 ± 0.3	n.d.	n.d.		

[1] MS counts were corrected for background via BSA controls and normalized. [2] n.d. represents no data, as the compound was not synthesized to generate affinity values. [3] Structures of the cations detected by MS.

affinities of these compounds ($1/K_d$, μM^{-1}) revealed a clear trend (Table 3a), which suggests that the amount of product formed is related to its affinity for the specific AChBP relative to those of the other members of the library. A similar correlation was observed when azide library **1b** (**9**–**13**) was screened against alkyne **3** (Table 3b). Under those conditions, triazole **18** was formed in the greatest amount by *Ls* and was also shown to have the highest affinity (K_d = 0.96 ± 0.22 nM), consistent with the observations from library **1a**. Pyrrolidinium derivative **19**, which was formed in lower amounts, had a significantly lower affinity (K_d = 82 ± 14 nM). In contrast, the amount of triazoles **16**, **17**, and **20**–**22** were comparatively low, and therefore, they were not synthesized. The capability to identify only combinations that warrant larger-scale synthesis and further investigation demonstrates another advantage of the in situ click chemistry approach.

After tropane derivative **18** had been identified as the compound of highest affinity, a set of alkynes was designed and reacted with azide **9**. This library, comprising the previously tested quinolinone derivative **3** and variously substituted aryl propargyl ethers **23**–**26** (Table 4), was incubated with the *Ls*, *Ac*, and *Ac*Y55W AChBPs. LC/MS analysis of the reaction mixtures (performed in triplicate) showed that all of the tested alkynes underwent AChBP-templated cycloaddition reactions with azide **9**. As before, the reactions against the BSA control produced no detectable products. Triazoles **27**–**29** were synthesized using standard CuAAC conditions, and their K_d values were determined (Table 5). Again it is worth noting that compounds **27**–**29** shared both comparable amounts of product formation and similar magnitudes of the affinity. Only triazole **30** was not synthesized in the presence of *Ac* or *Ac*Y55W AChBPs, and only small amounts were detected in the reaction catalyzed by *Ls*. The previously discovered triazole **18**, originating from alkyne **3** and azide **9**, was formed in significantly higher quantity and, as expected, exhibited a substantially higher affinity for all of the binding proteins (Table 5).

Table 4. Alkyne Library 2 Utilized for an in situ Click Chemistry Screen against Azide 9

Library	Azide	Alkynes				
2	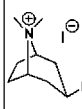	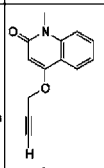	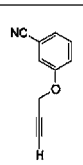	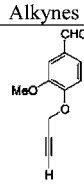	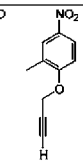	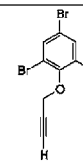
	9	**3**	**23**	**24**	**25**	**26**

Table 5. Templation and Binding Data for the Triazole Derivatives of the in situ Click Chemistry Screen of Alkyne Building Blocks (Library 2)

AChBP species	MS counts[1]	K_d [nM]	Affinity [μM^{-1}]	Structure[3]	#
Ls	100.0 ± 2.2	0.96 ± 0.22	1040	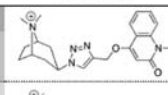	**18**
Ac	11.4 ± 0.4	24 ± 6.8	42		
*Ac*Y55W	10.3 ± 0.3	17 ± 4.8	59		
Ls	17.0 ± 0.2	42 ± 19	24	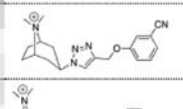	**27**
Ac	6.7 ± 0.3	220 ± 87	4.5		
*Ac*Y55W	6.2 ± 0.1	130 ± 35	7.7		
Ls	20.3 ± 0.4	64 ± 26	16	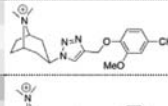	**28**
Ac	7.7 ± 0.5	260 ± 80	3.8		
*Ac*Y55W	11.3 ± 0.1	130 ± 44	7.7		
Ls	10.6 ± 0.6	13 ± 6.5	77	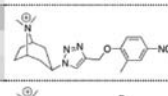	**29**
Ac	6.1 ± 0.4	61 ± 27	16		
*Ac*Y55W	4.2 ± 0.1	30 ± 18	33		
Ls	4.3 ± 0.1	n.d.[2]	n.d.	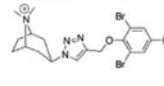	**30**
Ac	0.0	n.d.	n.d.		
*Ac*Y55W	0.0	n.d.	n.d.		

[1] MS counts were corrected for background via BSA controls and normalized. [2] n.d. represents no data, as the compound was not synthesized to generate affinity values. [3] Structures of the cations detected by MS.

Having demonstrated that AChBPs selectively catalyze the formation of high-affinity ligands from libraries of alkynes and azides, we next examined whether the template could select the most productive combinations (i.e., those resulting in the most potent ligands) from a pool of various azides and alkynes simultaneously present in the reaction mixture. To this end,

dx.doi.org/10.1021/ja3001858 | *J. Am. Chem. Soc.* 2012, 134, 6732–6740

azides **4**−**13** were reacted with alkynes **3** and **23**−**26** in a combined mixture using *Ls* as the template (see Experimental Methods for details). *Ls* was chosen because of the higher yields obtained in the previous reactions shown in Tables 3a, 3b, and 5. To compensate for the reduced concentrations of the individual building blocks, the incubation time was increased to 10 days. The results showed that several triazole products could be detected in comparison with the BSA control reaction, which exhibited no product formation (Figure 2).

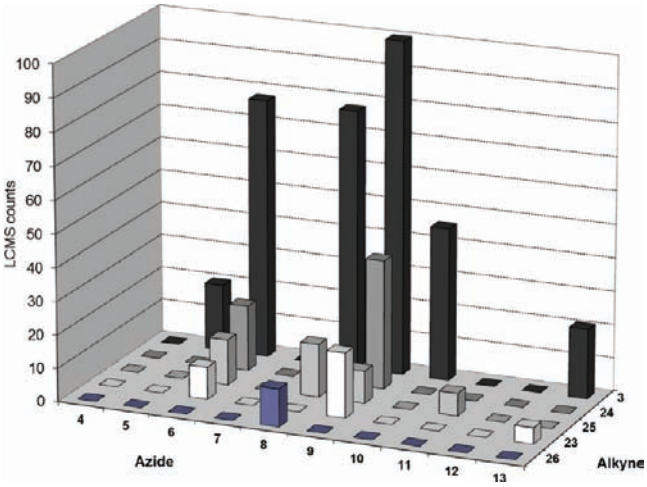

Figure 2. Templation data for the triazole derivatives of the in situ screen of azide and alkyne building blocks on *Ls* AChBP (data have been normalized to the largest peak).

The majority of the products formed in the presence of the *Ls* template had been previously identified in simpler in situ reaction pools. Triazole **18**, the product of the cycloaddition between alkyne **3** and azide **9**, was again formed in the greatest amounts, which is consistent with the affinity of this triazole for *Ls*. Compound **14**, with the second highest affinity discovered in this study, was formed in the second largest amount. Similar trends between the affinities of previously examined triazole products and the amounts formed were also observed, despite the increased complexity of the system. Interestingly, the combination of quinuclidinium azide **8** and alkynes **25** and **26** and the cycloaddition products of piperidinium azide **6** with alkynes **23**, **24**, and **25** were identified by LC/MS analysis. These products were the result of combinations that had not previously been screened. Although it is of note that these compounds formed in situ, the relatively low amounts formed suggests they have lower affinities and were therefore accorded lower priority.

We have therefore demonstrated that it is possible to screen libraries of azides and alkynes simultaneously and detect the formation of triazole products while generating valuable information regarding the affinity of the compounds for the target protein. The increased number of building blocks screened in a single reaction further increases the throughput of the in situ click chemistry approach. Moreover, the observed positive correlation between the amount of product formed and its affinity for the target could be useful for subsequent structure−activity studies, whether through traditional medicinal chemistry methods or further iterations of in situ target-templated screening.

Having demonstrated that triazole **18** exhibited the highest affinity of all the compounds detected throughout this study, we determined binding parameters of its 1,5-isomer, **18a**, which was prepared using RuAAC as shown in Scheme 2. Although

Scheme 2. RuAAC Synthesis of the 1,5-Triazole Isomer 18a

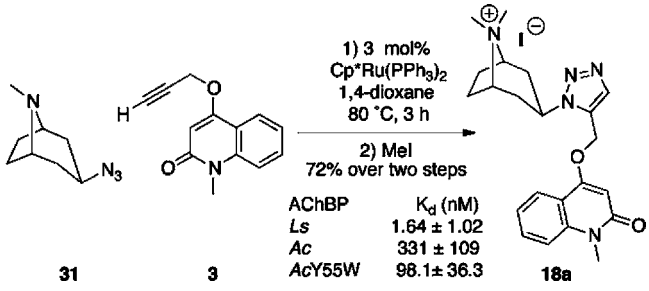

the K_d of **18a** for *Ls* was only slightly higher than of **18**, its binding to *Ac* and *AcY55W* was significantly weaker, thus other 1,5-disubstituted triazoles were not examined further in the present study.

To define the binding site determinants governing the reaction, we were interested in deciphering the binding pose of triazole **18**, the most potent ligand found in this study. Since our conditions of crystallization typically yielded higher-resolution structures with *Ac* AChBP, we concentrated on refining the structure of this complex, yielding a structure with a resolution of 2.3 Å. The 3σ omit map of the best represented ligand is shown in Figure 3A.

We found the density for the quinolinone to be much weaker than that of the triazole and tropane ring systems in most of the binding sites. The faint density suggests a flexibility of the quinolinone that is most likely due to the rotatable methylene carbon bond that links the quinolinone to the triazole. Indeed, the binding mode shows that the quaternary-bridged-nitrogen forms cation−π interactions with the Trp147, Tyr188, and Tyr93 side chains, a previously noted observation for quaternary amines that bind nAChRs.[38] Figure 3B and Supplementary Figure 1C in the Supporting Information show the distances between the quaternary tropane nitrogen and the closest atoms in the aromatic side chains of Trp147, Tyr93, and Tyr188 to be between 4.3 and 5.2 Å, as has been noted to be optimal for cation−π interactions.[43] The tight fit of the ligand is achieved by the aromatic side chains, including Y195 from the principal subunit and Y55 from the complementary subunit, which surround the quaternary nitrogen and provide an anchor for the azide building block **9** (Figure 3C). The propargyloxyquinolinone ring system stacks between the vicinal disulfide bridge joining Cys190 and Cys191 of the β9−β10 linker (loop C) and Met116 (Figure 3B,D and Supplementary Figure 1B). The triazole is positioned such that N3 forms a hydrogen bond with a neighboring water molecule, similar to that reported for the pyridine ring systems (Figure 3B and Supplementary Figure 1A).[37,39,44] This water molecule forms a hydrogen-bond linkage with other water molecules extending toward the complementary subunit and the vestibule of the nAChR channel. The ether oxygen also forms a hydrogen-bonding system with Arg79 and Tyr195. The hydroxyl of Tyr195 approaches basally, while the protonated nitrogen of Arg79 reaches down from the apical region. The carbonyl of Val148, which binds to the complementary hydrogen of Arg79's protonated nitrogen, and a structural water associated between Tyr195 and Glu193 completes the hydrogen-bonding system (Supplementary Figure 1A).

dx.doi.org/10.1021/ja3001858 | *J. Am. Chem. Soc.* 2012, 134, 6732−6740

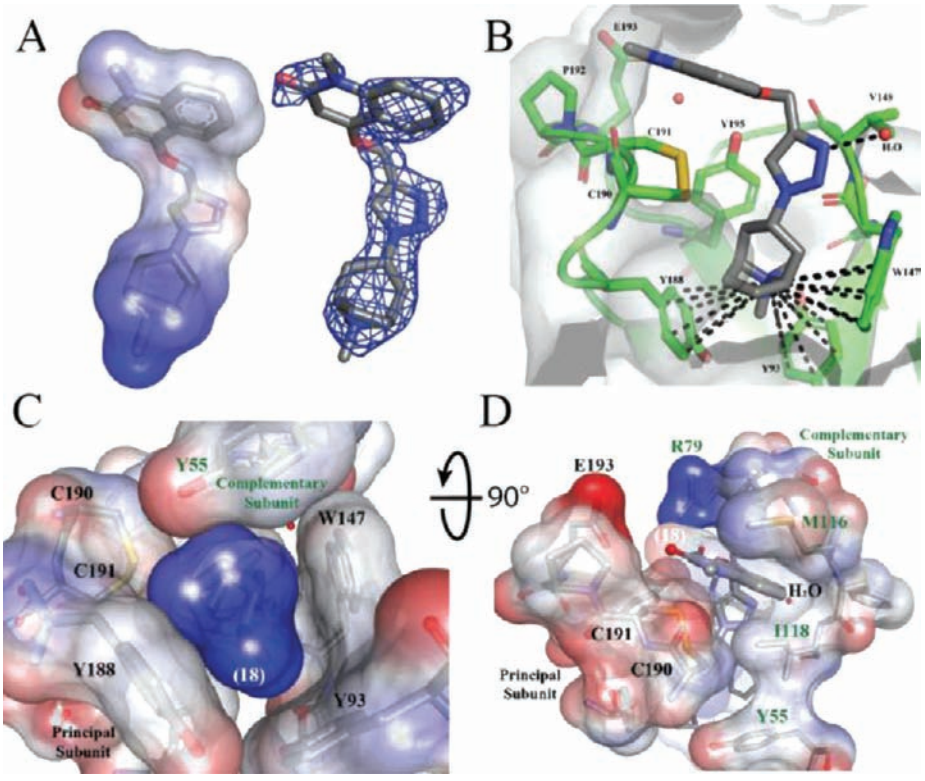

Figure 3. Crystallographic analysis of triazole **18** in complex with *Ac* AChBP. The complementary subunit is represented with green labels, while the primary subunit is denoted with black labels. (A) Surface representation of ligand interpolated charges and the $F_o - F_c$ omit map at 3σ. (B) Triazole **18** in the principal subunit binding pocket highlights the interactions of the dimethyltropane aza nitrogen with the surrounding aromatic residues Trp147, Tyr93, and Tyr188 in the principal subunit, viewed radially at the subunit interface. The interaction of the triazole nitrogen (N3) with a structural water is also shown. Residues shown are within 4 Å. (C) Connolly surface representation of the quaternary tropane moiety as viewed from the membrane side of the binding site. Stabilization is achieved by the aromatic nest of residues of the principal subunit noted in (B) and Tyr55 from the complementary subunit. (D) Surface representation of the quinolinone, triazole, and tropane rings (dark gray sticks, white label) showing the participation of Arg79, Met116, Ile118, and Tyr55 of the complementary subunit in addition to those noted in the principal subunit.

4. DISCUSSION

In situ click chemistry has previously been employed in the development of high-affinity ligands for the active sites of acetylcholinesterase, HIV protease, and carbonic anhydrase.[18,41,45,46] These ligands bind within a gorge centrosymmetric to a subunit in the oligomeric AChE, the shallow binding site in the HIV protease, or the single subunit in monomeric carbonic anhydrase, respectively. The AChBPs, with their binding sites at the interface of two subunits, provide a distinct template for in situ click chemistry, yet the bioorthogonal reaction forming the heterocyclic triazole can take place in the presumably more flexible and exposed subunit interface.

In this study, we have also demonstrated that the efficiency of the target-catalyzed synthesis of the ligands is partially determined by the affinity of the reaction product, that is, the amount of the formed triazole increases with the strength of its binding to the target. This was also the case when we compared the preference of *anti* and *syn* regioisomer formation on acetylcholinesterase with the equilibrium affinities of the respective triazoles.[47] This correlation between preference of formation and equilibrium affinity may suggest that the transition state more closely resembles the reaction product than the simple bimolecular associations of the building blocks with the template.

With the acetylcholinesterase complexes, we demonstrated that the higher-affinity *syn* regioisomer of the triazole induced a change in conformation that enhanced aromatic $\pi-\pi$ association at the peripheral site, whereas a change in conformation did not occur with the lower affinity *anti* isomer.[19] Accordingly, one of the tenets of selectivity for the in situ click chemistry reaction may arise from the precursors driving a conformation preferred by the triazole reaction product rather than accommodating a conformation of the unbound protein. This bodes well for the ability of the technique to select conformations of the ligand–protein complex that differ from the unbound protein.

Further support for the concept that the triazole product adopts a binding pose and selects a conformation most compatible with the product association comes from an examination of the crystal structure of triazole **18**. Here we observe a bound conformation and pose that has been predicted from the conformation of other quaternary-amine-containing ligands that bind to AChBP through cation–quadrupole interactions involving the electron-rich aromatic side chains (e.g., tryptophan). The positioning of the triazole such that it may form a hydrogen bond within the pocket supports the notion that precursors drive a conformation change needed for the reaction between them. The in situ reaction may be influenced by the binding strength of the component containing the tertiary or quaternary nitrogen (in our case, the quaternary tropane) and the ability of the complementary component to form the triazole in the proper orientation to allow for the formation of a highly selective

dx.doi.org/10.1021/ja3001858 | J. Am. Chem. Soc. 2012, 134, 6732–6740

molecule. Comparison of precursor component conformations with those of the final triazole compound will be of interest in the future. However, accomplishing this task may be difficult, as the precursor affinities are typically low, so their crystal structures would not be well-resolved in the pocket of the AChBP.

5. CONCLUSIONS

We have successfully used a combination of CuAAC and in situ click chemistry to achieve rapid conversion of the endogenous ligand of nAChRs, acetylcholine, into compound **18**, a highly potent and selective ligand for *Ls* AChBP. This work represents the first example of in situ click chemistry performed at a flexible subunit interface of an oligomeric protein and thus increases the number of biologically relevant targets that can be investigated using this methodology. In addition, we have demonstrated a positive correlation between the amount of product generated in situ and its affinity for the target binding protein. Therefore, this approach enables rapid refinement of structures while providing valuable information about binding and selectivity over closely related targets without the need to synthesize and assay individual compounds. Furthermore, we have shown that sets of building blocks can be screened in a single reaction pool with 10 azides and 5 alkynes, allowing for the possible generation and detection of the highest-affinity compounds from several discrete sets of congeneric building blocks. The variety of possible combinations enhances the efficiency of the technique and reduces the amount of protein required for the experiments. Finally, we have cocrystallized the most active compound that emerged from these studies, **18**, with *Ac*-AChBP and shown that our initial hypothesis about specific interactions was indeed valid. We are currently continuing to expand the utility of the combination of these methodologies for further refinement of our lead molecules for both affinity and selectivity toward *Ls* AChBP and subsequently investigating whether these properties can translate the ligand's affinity to human nAChRs. Historically, the AChBPs have provided significant insights into the determinants of ligand recognition by nAChRs. In particular, crystal structures of *Ls*– and *Ac*–ligand complexes have elucidated and confirmed residues involved in the ligand binding domain as well as given rise to information regarding the global extracellular domain. It has also been possible to modify the side chains of AChBP so that its subunit interface more closely resembles that of the homomeric α7 nAChR.[48] This target-templated ligand identification approach, coupled with a multiarray synthesis of triazoles from azide and alkyne building blocks, offers an efficient means of identifying and then refining candidate ligands specifically engineered toward the nAChRs and other flexible targets.

■ ASSOCIATED CONTENT

Supporting Information

Synthetic methods, characterization of new compounds, and additional data on the crystallographic analysis of the *Ac* AChBP cocrystallized with triazole **18**. This material is available free of charge via the Internet at http://pubs.acs.org.

■ AUTHOR INFORMATION

Corresponding Author

fokin@scripps.edu

Notes

The authors declare no competing financial interest.

■ ACKNOWLEDGMENTS

This study was supported by USPHS Grants UO1 DA19320-05 and R01 GM18360-37. B.S. acknowledges a fellowship from the Swiss National Science Foundation (SNF). J.G.Y. and Á.N. were supported by NIH Training Grant GM-07752. J.G.Y. was also supported by NSF Grant GK-12 0742551. C.K. was supported by NIH Grant R01 GM090161-01 and a Robert A. Welch Foundation Chemistry and Biology Collaborative Grant. V.V.F. acknowledges support by NIH (NIGMS) Grant R01 GM087620. The Berkeley Center for Structural Biology is supported in part by the National Institutes of Health, National Institute of General Medical Sciences, and the Howard Hughes Medical Institute. The Advanced Light Source is supported by the Director, Office of Science, Office of Basic Energy Sciences, of the U.S. Department of Energy under Contract DE-AC02–05CH11231.

■ REFERENCES

(1) Karlin, A. *Nat. Rev. Neurosci.* **2002**, *3*, 102.
(2) Changeux, J. P.; Taly, A. *Trends Mol. Med.* **2008**, *14*, 93.
(3) Thompson, A. J.; Lester, H. A.; Lummis, S. C. *Q. Rev. Biophys.* **2010**, *43*, 449.
(4) Changeux, J. P.; Edelstein, S. J. *Nicotinic Acetylcholine Receptors: From Molecular Biology to Cognition*; Odile Jacob/Johns Hopkins University Press: New York, 2005.
(5) Changeux, J. P. *Nat. Rev. Neurosci.* **2010**, *11*, 389.
(6) Vernallis, A. B.; Conroy, W. G.; Berg, D. K. *Neuron* **1993**, *10*, 451.
(7) Smit, A. B.; Syed, N. I.; Schaap, D.; van Minnen, J.; Klumperman, J.; Kits, K. S.; Lodder, H.; van der Schors, R. C.; van Elk, R.; Sorgedrager, B.; Brejc, K.; Sixma, T. K.; Geraerts, W. P. *Nature* **2001**, *411*, 261.
(8) Hansen, S. B.; Talley, T. T.; Radic, Z.; Taylor, P. *J. Biol. Chem.* **2004**, *279*, 24197.
(9) Celie, P. H.; Klaassen, R. V.; van Rossum-Fikkert, S. E.; van Elk, R.; van Nierop, P.; Smit, A. B.; Sixma, T. K. *J. Biol. Chem.* **2005**, *280*, 26457.
(10) Huang, J.; Wang, H.; Cui, Y.; Zhang, G.; Zheng, G.; Liu, S.; Xie, L.; Zhang, R. *Mar. Biotechnol.* **2009**, *11*, 596.
(11) McCormack, T.; Petrovich, R. M.; Mercier, K. A.; DeRose, E. F.; Cuneo, M. J.; Williams, J.; Johnson, K. L.; Lamb, P. W.; London, R. E.; Yakel, J. L. *Biochemistry* **2010**, *49*, 2279.
(12) Brejc, K.; van Dijk, W. J.; Klaassen, R. V.; Schuurmans, M.; van Der Oost, J.; Smit, A. B.; Sixma, T. K. *Nature* **2001**, *411*, 269.
(13) Furlan, R. L. E.; Otto, S.; Sanders, J. K. M. *Proc. Natl. Acad. Sci. U.S.A.* **2002**, *99*, 4801.
(14) Rideout, D. *Cancer Invest.* **1994**, *12*, 189.
(15) Rideout, D.; Calogeropoulou, T.; Jaworski, J.; McCarthy, M. *Biopolymers* **1990**, *29*, 247.
(16) Eliseev, A. V. *Pharm. News* **2002**, *9*, 207.
(17) Tomé, A. C. *Sci. Synth.* **2003**, *13*, 544.
(18) Lewis, W. G.; Green, L. G.; Grynszpan, F.; Radic, Z.; Carlier, P. R.; Taylor, P.; Finn, M. G.; Sharpless, K. B. *Angew. Chem., Int. Ed.* **2002**, *41*, 1053.
(19) Bourne, Y.; Kolb, H. C.; Radic, Z.; Sharpless, K. B.; Taylor, P.; Marchot, P. *Proc. Natl. Acad. Sci. U.S.A.* **2004**, *101*, 1449.
(20) Rostovtsev, V. V.; Green, L. G.; Fokin, V. V.; Sharpless, K. B. *Angew. Chem., Int. Ed.* **2002**, *41*, 2596.
(21) Tornoe, C. W.; Christensen, C.; Meldal, M. *J. Org. Chem.* **2002**, *67*, 3057.
(22) Majumdar, K. C.; Ghosh, M.; Jana, M. *Synthesis* **2002**, 669.
(23) Zhang, L.; Chen, X.; Xue, P.; Sun, H. H. Y.; Williams, I. D.; Sharpless, K. B.; Fokin, V. V.; Jia, G. *J. Am. Chem. Soc.* **2005**, *127*, 15998.

(24) Boren, B. C.; Narayan, S.; Rasmussen, L. K.; Zhang, L.; Zhao, H.; Lin, Z.; Jia, G.; Fokin, V. V. *J. Am. Chem. Soc.* **2008**, *130*, 8923.
(25) Hansen, S. B.; Sulzenbacher, G.; Huxford, T.; Marchot, P.; Taylor, P.; Bourne, Y. *EMBO J.* **2005**, *24*, 3635.
(26) Talley, T. T.; Yalda, S.; Ho, K. Y.; Tor, Y.; Soti, F. S.; Kem, W. R.; Taylor, P. *Biochemistry* **2006**, *45*, 8894.
(27) Reeves, P. J.; Callewaert, N.; Contreras, R.; Khorana, H. G. *Proc. Natl. Acad. Sci. U.S.A.* **2002**, *99*, 13419.
(28) Cheng, Y.; Prusoff, W. H. *Biochem. Pharmacol.* **1973**, *22*, 3099.
(29) Otwinowski, Z.; Minor, W. *Methods Enzymol.* **1997**, *276*, 307.
(30) Storoni, L. C.; McCoy, A. J.; Read, R. J. *Acta Crystallogr., Sect. D* **2004**, *60*, 432.
(31) Emsley, P.; Cowtan, K. *Acta Crystallogr., Sect. D* **2004**, *60*, 2126.
(32) Murshudov, G. N.; Vagin, A. A.; Dodson, E. J. *Acta Crystallogr., Sect. D* **1997**, *53*, 240.
(33) DeLano, W. L. *The PyMOL Molecular Graphics System*; DeLano Scientific: San Carlos, CA, 2002.
(34) Horne, W. S.; Stout, C. D.; Ghadiri, M. R. *J. Am. Chem. Soc.* **2003**, *125*, 9372.
(35) Van Maarseveen, J. H.; Horne, W. S.; Ghadiri, M. R. *Org. Lett.* **2005**, *7*, 4503.
(36) Angell, Y. L.; Burgess, K. *Chem. Soc. Rev.* **2007**, *36*, 1674.
(37) Celie, P. H.; van Rossum-Fikkert, S. E.; van Dijk, W. J.; Brejc, K.; Smit, A. B.; Sixma, T. K. *Neuron* **2004**, *41*, 907.
(38) Xiu, X.; Puskar, N. L.; Shanata, J. A.; Lester, H. A.; Dougherty, D. A. *Nature* **2009**, *458*, 534.
(39) Hibbs, R. E.; Sulzenbacher, G.; Shi, J.; Talley, T. T.; Conrod, S.; Kem, W. R.; Taylor, P.; Marchot, P.; Bourne, Y. *EMBO J.* **2009**, *28*, 3040.
(40) Bourne, Y.; Radic, Z.; Araoz, R.; Talley, T. T.; Benoit, E.; Servent, D.; Taylor, P.; Molgo, J.; Marchot, P. *Proc. Natl. Acad. Sci. U.S.A.* **2010**, *107*, 6076.
(41) Mamidyala, S. K.; Finn, M. G. *Chem. Soc. Rev.* **2010**, *39*, 1252.
(42) While mass spectrometry cannot give a quantitative measurement of the amount of product formed, our investigations demonstrate that qualitative relationships can be ascertained (see the Supporting Information for details).
(43) Scharer, K.; Morgenthaler, M.; Paulini, R.; Obst-Sander, U.; Banner, D. W.; Schlatter, D.; Benz, J.; Stihle, M.; Diederich, F. *Angew. Chem., Int. Ed.* **2005**, *44*, 4400.
(44) Talley, T. T.; Harel, M.; Hibbs, R. E.; Radic, Z.; Tomizawa, M.; Casida, J. E.; Taylor, P. *Proc. Natl. Acad. Sci. U.S.A.* **2008**, *105*, 7606.
(45) Mocharla, V. P.; Colasson, B.; Lee, L. V.; Roeper, S.; Sharpless, K. B.; Wong, C.-H.; Kolb, H. C. *Angew. Chem., Int. Ed.* **2005**, *44*, 116.
(46) Whiting, M.; Muldoon, J.; Lin, Y.-C.; Silverman, S. M.; Lindstrom, W.; Olson, A. J.; Kolb, H. C.; Finn, M. G.; Sharpless, K. B.; Elder, J. H.; Fokin, V. V. *Angew. Chem., Int. Ed.* **2006**, *45*, 1435.
(47) Bourne, Y.; Radic, Z.; Taylor, P.; Marchot, P. *J. Am. Chem. Soc.* **2010**, *132*, 18292.
(48) Nemecz, A.; Taylor, P. W. *J. Biol. Chem* **2011**, *286*, 42555.